

# Picosecond pump pulses probe the relevance of hot electrons for the laser-induced phase transition in FeRh

M. Mattern,<sup>1</sup> S. P. Zeuschner,<sup>1</sup> J. A. Arregi,<sup>2</sup> V. Uhlř,<sup>2,3</sup> and M. Bargheer<sup>1,4</sup>

<sup>1</sup>*Institut für Physik und Astronomie, Universität Potsdam, 14476 Potsdam, Germany*

<sup>2</sup>*CEITEC BUT, Brno University of Technology, 61200 Brno, Czech Republic*

<sup>3</sup>*Institute of Physical Engineering, Brno University of Technology, 61669 Brno, Czech Republic*

<sup>4</sup>*Helmholtz-Zentrum Berlin für Materialien und Energie GmbH, Wilhelm-Conrad-Röntgen Campus, BESSY II, 12489 Berlin, Germany<sup>a)</sup>*

(Dated: 30 October 2023)

Recent ultrafast photoemission experiments showed signatures of an ultrafast modification of the electronic band structure in FeRh indicative of a ferromagnetic (FM) state that is initiated by a non-equilibrium occupation of the electronic states upon femtosecond laser excitation. We use ultrafast x-ray diffraction to examine the impact of hot electrons on the antiferromagnetic (AFM) to FM phase transition. By increasing the pump-pulse duration up to 10.5 ps, we eliminate hot electrons and see that the nucleation of FM domains still proceeds at the intrinsic timescale of 8 ps, which starts when the deposited energy surpasses the threshold energy. For long pulses, the phase transition proceeds considerably faster than predicted by a convolution of the dynamics observed for ultrafast excitation with the long pump pulse duration. We predict that quite generally, slow photoexcitation can result in a fast response, if the non-linear threshold behavior of a first-order phase transition is involved.

First-order phase transitions are characterized by an abrupt change of structural, electronic or/and magnetic properties and a co-existence of multiple phases when the deposited energy in thermal equilibrium<sup>1–4</sup> or on ultrafast timescales<sup>5–12</sup> exceeds a threshold. The abruptly emerging phase is a consequence of a fine interplay of spin, charge and lattice degrees of freedom<sup>6,13</sup>. Since the optical excitation often affects only the electrons directly, they heat up far beyond the transition temperature, rendering the driving mechanism of the laser-induced phase transition a formidable question.

Since the discovery of the first-order magneto-structural antiferromagnetic-to-ferromagnetic (AFM-FM) phase transition of FeRh at 370 K different mechanisms such as expansion-induced sign change of the exchange constant<sup>14</sup>, excitation of spin waves<sup>15</sup> and dominant FM exchange of the Fe moments mediated by an induced Rh moment<sup>8,13,16–19</sup> were proposed.

On ultrafast timescales, direct signatures of the ferromagnetic phase transition of FeRh are the rise of the increased FM lattice constant<sup>10,11,20,21</sup> and the emergence of a net magnetization<sup>8,9,22–24</sup>. While the rise of the magnetization is most significant after the coalescence of the nucleated FM domains<sup>22–24</sup>, probing the structural order parameter via ultrafast x-ray diffraction (UXRD) directly yields insights into their nucleation and growth<sup>10,11,20,21</sup>, where the intrinsic nucleation time<sup>11</sup> of 8 ps applies for a wide range of fluences, external magnetic fields and even for FeRh nanostructures<sup>21</sup>.

The local configuration of magnetic moments has been described as a competition between bilinear and

higher-order four spin exchange terms in atomistic spin dynamics<sup>18</sup>, a combination of Heisenberg exchange of Fe and a Stoner model for Rh<sup>8</sup> and a modification of the Rh-Fe hybridization<sup>13,17,19</sup>. Recently, time-resolved photoelectron spectroscopy identified a sub-picosecond formation of an electronic ferromagnetic state<sup>19</sup>, related to a photo-induced change of the band structure: Charge transfer from Rh to Fe and an intersite spin transfer between Fe sites was found to induce a Rh moment during the relaxation of optically excited non-equilibrium electrons. However, it remains unclear if the non-equilibrium character of the photoexcited electrons is required for the laser-induced phase transition.

Here, we investigate the role of hot electrons concomitant with ultrashort laser pulse excitation for this prototypical phase transition. By ultrafast x-ray diffraction (UXRD), we directly measure how the kinetics of domain nucleation and the threshold of the AFM-FM phase transition depend on the duration of optical pump-pulses. For 10.5 ps-long pulses, the pronounced electron-phonon non-equilibrium present upon femtosecond laser excitation is effectively suppressed. Thus, we gradually deposit the energy in all subsystems and recover the energy threshold for the laser-induced phase transition known from equilibrium. The transient FM volume fraction extracted from the laser-induced strain response is found to exclusively depend on the total deposited energy. It reaches the same final value at the intrinsic nucleation timescale irrespective of the pump-pulse duration. As a consequence of the non-linear threshold behavior, the rise of the FM phase is delayed but faster than the convolution of the pump pulse duration with the signal upon femtosecond pulse excitation. In total, a laser-induced hot Fermi-distribution is not necessary to drive the phase

<sup>a)</sup>Electronic mail: [bargheer@uni-potsdam.de](mailto:bargheer@uni-potsdam.de)

transition on the intrinsic nucleation timescale.

Figure 1(a) sketches the epitaxial 12.6 nm thick FeRh(001) film grown by magnetron sputtering from an equiatomic FeRh target<sup>25</sup> on an MgO(001) substrate. We used synchrotron radiation from the KMC-3 XPP endstation at BESSY II<sup>26</sup> to determine the film thickness via x-ray reflectivity (XRR) and to characterize the first order AFM-FM phase transition via the concomitant change of the mean out-of-plane lattice constant  $d$  (symbols in Fig. 1(b)). The hysteresis for this locally probed lattice constant is narrower than the global temperature-dependent magnetization  $M_{\text{FeRh}}$  (solid line) determined by Vibrating sample magnetometry (VSM) using a QuantumDesign VersaLab magnetometer. The magnetization data indicates the presence of a residual FM phase of around 20 % originating from interface effects<sup>27–29</sup> consistent with the reduced out-of-plane expansion of  $\eta_{\text{AFM-FM}}^{\text{thin}} = 0.48\%$  compared to  $\eta_{\text{AFM-FM}}^{\text{thick}} = 0.6\%$  observed in thicker films<sup>11,21</sup>.

Figure 1(c) illustrates the influence of increasing the pump-pulse duration on the optically induced electron-phonon non-equilibrium. We model the transient mean electron  $T_{\text{el}}$  and phonon  $T_{\text{ph}}$  temperature of the FeRh film as function of the pump-pulse duration in the framework of a diffusive two-temperature model<sup>30</sup>. We use the modular PYTHON library UDKM1DSIM<sup>31</sup> and literature values for the Sommerfeld constant<sup>32</sup>  $\gamma^S = 0.06 \text{ J kg}^{-1} \text{ K}^{-2}$ , the phononic heat capacity<sup>33</sup>  $C_{\text{ph}} = 350 \text{ J kg}^{-1} \text{ K}^{-1}$  and the electron-phonon coupling constant<sup>34</sup>  $g^{\text{el-ph}} = 9 \cdot 10^{13} \text{ J kg}^{-1} \text{ K}^{-1}$ . The thermophysical properties of the MgO substrate were used as reported previously<sup>11</sup>. The excitation by a 60 fs pump pulse increases the electron temperature that stays significantly higher than the slowly rising phonon temperature within the first 3 ps, with the maximum  $\Delta T_{\text{el}}^{\text{max}} \approx 7 \Delta T_{\text{ph}}^{\text{max}}$ . Increasing the pump pulse duration to 2.9 ps drastically reduces the maximum electron temperature, as a considerable amount of energy already dissipated to the phonons during the optical deposition. For a pump pulse of duration 10.5 ps, the electron temperature barely exceeds the phonon temperature. A strong electron-phonon non-equilibrium with a substantial amount of hot electrons is absent.

In the following, we experimentally apply such pump-pulses to investigate the kinetics of the laser-induced phase transition in FeRh by UXRD. The thin film is excited by p-polarized pump pulses with a central wavelength of 800 nm that are incident under  $40^\circ$  with respect to the sample normal. We probe the transient out-of-plane strain response of the FeRh layer via symmetric  $\theta - 2\theta$  scans<sup>35</sup> around the FeRh(002) Bragg peak at our table-top laser-driven plasma x-ray source<sup>36</sup> providing 200 fs hard x-ray pulses with a photon energy of approx. 8 keV. The Bragg peak position along the reciprocal space coordinate  $q_z$  encodes the mean out-of-plane lattice constant  $d$  of the FeRh films via  $q_z = 4\pi/d$ . The lattice strain  $\eta_{\text{FeRh}} = \Delta d/d_0$  is the relative change  $\Delta d$  of the lattice constant with respect to its value  $d_0$  before ex-

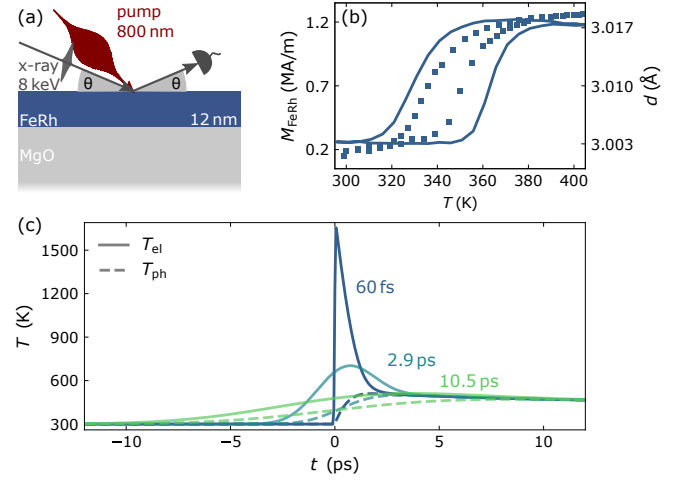
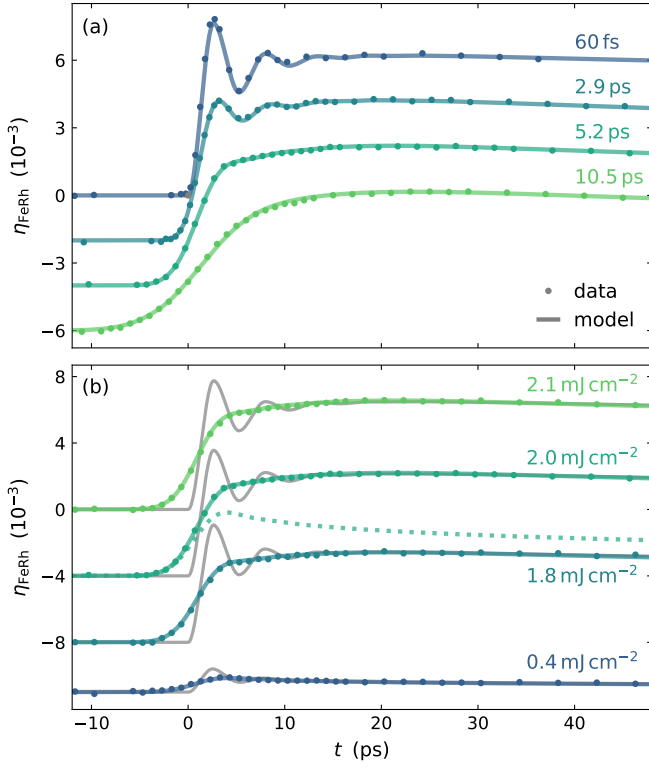


FIG. 1. **Long pump-pulses suppress electron-phonon non-equilibrium:** (a) Sketch of the thin film sample and the UXRD experiment, mapping the reciprocal space via  $\theta - 2\theta$  scans. (b) Characterization of the AFM-FM phase transition in equilibrium by the magnetization (solid line) and the mean out-of-plane lattice constant  $d$  (symbols). (c) Modelled transient electron and phonon temperature upon excitation by pump-pulses of various durations for a fluence of  $2.0 \text{ mJ cm}^{-2}$ .

citation. We independently determined the pump-probe overlap and calibrated the duration of the pump-pulse by the strictly linear laser-induced response of a metal-insulator superlattice serving as reference sample<sup>36</sup>.

Figure 2(a) displays the laser-induced strain response of the thin FeRh film for a fluence of  $2.0 \text{ mJ cm}^{-2}$  and different pump pulse durations ranging from 60 fs to 10.5 ps. The excitation fluence exceeds the previously identified critical threshold<sup>11</sup> of  $F_{\text{th}} = 0.6 \text{ mJ cm}^{-2}$  for this sample at room temperature and drives the magnetostructural phase transition that is associated with an out-of-plane expansion of FeRh. In total, the strain response is the superposition of an expansion due to the phase transition, a quasi-static expansion due to heating and a propagating strain pulse reflected at the surface and the FeRh-MgO interface, where it is partially transmitted into the substrate. In case of the excitation by a 60 fs pulse, this results in a decaying oscillation<sup>30</sup> with a period of  $2L_{\text{FeRh}}/v_s = 5 \text{ ps}$  given by the layer thickness  $L_{\text{FeRh}}$  and the sound velocity  $v_s = 5 \text{ nm ps}^{-1}$ <sup>137</sup> (see Figure 2(a)). Increasing the pump-pulse duration successively suppresses this oscillation of the mean out-of-plane strain until 10.5 ps pump-pulses only drive a slow expansion. The strain at 40 ps is identical for all pump-pulse durations. This indicates that all strain contributions including the expansion associated with the AFM-FM phase transition exclusively depend on the deposited energy and not on the details of the optical excitation.

Fig. 2(b) compares the transient strain for pump pulse durations of 5 ps (symbols) and 60 fs (grey solid curves) for various super- and sub-threshold fluences. At first sight, the long pump pulses seem just to smear out the



**FIG. 2. Transient strain response contains expansion from phase transition:** The laser-induced out-of-plane expansion of FeRh for various pump-pulse durations at the constant fluence  $2 \text{ mJ cm}^{-2}$  (a) and as function of the fluence for the constant pulse duration  $5.2 \text{ ps}$  pump-pulses (b). The grey solid lines denote the modelled strain response for the respective fluence driven by femtosecond laser excitation reproduced as reference from a previous publication<sup>11</sup>. The colored solid lines in (a) and (b) display the model described in the text, which adds the fluence-scaled strain response to  $F_{\text{st}} = 0.4 \text{ mJ cm}^{-2}$  convoluted with the respective pump-pulse to the expansion  $\eta_{\text{AFM-FM}}^{\text{thin}} \Delta V_{\text{FM}}(t)$  associated with the phase transition.  $\Delta V_{\text{FM}}(t)$  is plotted in Fig. 3. The results are offset for clarity.

oscillations resulting from coherent longitudinal acoustic phonons. We obtain better insight by disentangling the linear acoustic response of the sample from the expansion driven by the phase transition, which depends non-linearly on the excitation fluence. The sub-threshold fluence of  $F_{\text{bt}} = 0.4 \text{ mJ cm}^{-2}$  does not induce the AFM-FM phase transition<sup>11</sup>. This simplifies the strain response to a superposition of a quasi-static expansion and propagating strain pulses, which both depend linearly on the deposited pulse energy. Therefore, the acoustic strain contribution upon a super-threshold excitation is given by this sub-threshold strain response  $\eta_{\text{FeRh}}^{\text{bt}}$  (grey solid line) scaled by the ratio of the fluences  $s = F_{\text{at}}/F_{\text{bt}}$  and convoluted with the respective pump-pulse duration.

The dotted line in Fig. 2(b) depicts the acoustic strain contribution for  $F_{\text{at}} = 2 \text{ mJ cm}^{-2}$  given by  $s \cdot \eta_{\text{FeRh}}^{\text{bt}}$  with  $s = 5$ . The deviation  $\Delta\eta(t) = \eta_{\text{FeRh}}^{\text{at}} - s \cdot \eta_{\text{FeRh}}^{\text{bt}}$  from the

strain response to the super-threshold excitation  $\eta_{\text{FeRh}}^{\text{at}}$  is essentially due to the additional expansion induced by the phase transition, which directly provides insights into the rise of the FM volume fraction  $V_{\text{FM}}(t)$ . To determine its absolute value, we consider the residual FM phase  $V_{\text{FM}}^0 = 0.2$  present before the laser excitation due to interface effects and the latent heat  $C_{\text{AFM-FM}}$  of the first-order phase transition. The energy  $Q_{\text{AFM-FM}} = \int C_{\text{AFM-FM}} dT$  required for transforming FeRh into the FM phase reduces the local temperature<sup>38</sup> by  $\Delta T = Q_{\text{AFM-FM}}/C_{\text{ph}}$ , which reduces the quasi-static expansion of FeRh by  $\eta_{\text{AFM}} = \alpha_{\text{AFM}} \Delta T$  with the expansion coefficient  $\alpha_{\text{AFM}}$  in the AFM phase. This relates the deviation in the transient strain  $\Delta\eta(t)$  to the laser-induced FM volume fraction  $\Delta V_{\text{FM}}$  via:

$$\Delta\eta(t) = (\eta_{\text{AFM-FM}}^{\text{thick}} - \eta_{\text{AFM}}) \Delta V_{\text{FM}}(t). \quad (1)$$

Figure 3 displays the laser-induced volume fraction  $\Delta V_{\text{FM}}$  derived from the measured transient strain via Eq. (1). The variation of the excitation fluence in Fig. 3(b) exemplifies the non-linear response at the phase transition: A tiny increase of the fluence from  $1.8$  to  $2.1 \text{ mJ cm}^{-2}$  changes  $\Delta V_{\text{FM}}$  from  $60\%$  to a complete phase transition, which corresponds to  $\Delta V_{\text{FM}} = 80\%$ . The data for  $60 \text{ fs}$  pulse excitation in Fig. 3(a) is very well reproduced by the nucleation of domains on a  $\tau = 8 \text{ ps}$  timescale by<sup>30</sup>:

$$\Delta V_{\text{FM}}(t) = \mathcal{H}(t) V_{\text{FM}}^* \cdot (1 - e^{-t/\tau}), \quad (2)$$

with the Heaviside function  $\mathcal{H}(t)$  and the final FM volume fraction increase  $V_{\text{FM}}^*$  that depends on the fluence with  $V_{\text{FM}}^* > 0$  if  $F > F_{\text{th}}$  and  $V_{\text{FM}}^* = 0.8$  if  $F = 2.1 \text{ mJ cm}^{-2}$  as reported previously<sup>11</sup>.

Equation (2) yields excellent agreement with  $\Delta V_{\text{FM}}$  for  $60 \text{ fs}$  in Fig. 3(a). As a first attempt, the dashed lines for the longer pump-pulses in Fig. 3 represent  $\Delta V_{\text{FM}}(t)$  from Eq. (2) convoluted with a Gaussian representing the pump-pulse in the experiment. However, the deviation of the measured transient FM volume fraction from this simple estimation becomes larger with increasing pump-pulse duration (see Fig. 3(a)). Interestingly, the data rise faster than the convolution although the rise starts later, which must be a consequence of the non-linearity associated with the threshold for the phase transition.

As an improved model of the rising  $\Delta V_{\text{FM}}$  for long pump-pulses, we explicitly consider the successively deposited energy that leads to the unlocking of the AFM-FM phase transition in an increasing volume fraction of the film during the pump-pulse. This explicit treatment of the threshold character of first-order phase transitions extends Eq. (2) in the case of picosecond pump-pulses to:

$$\Delta V_{\text{FM}}(t) = \int \mathcal{H}(t - t') V_{\text{FM}}^*(t') \cdot (1 - e^{-(t-t')/\tau}) dt'. \quad (3)$$

Here, the FM volume fraction  $V_{\text{FM}}^*(t')$  is unlocked at delay  $t'$  by the increase of the deposited energy and rises

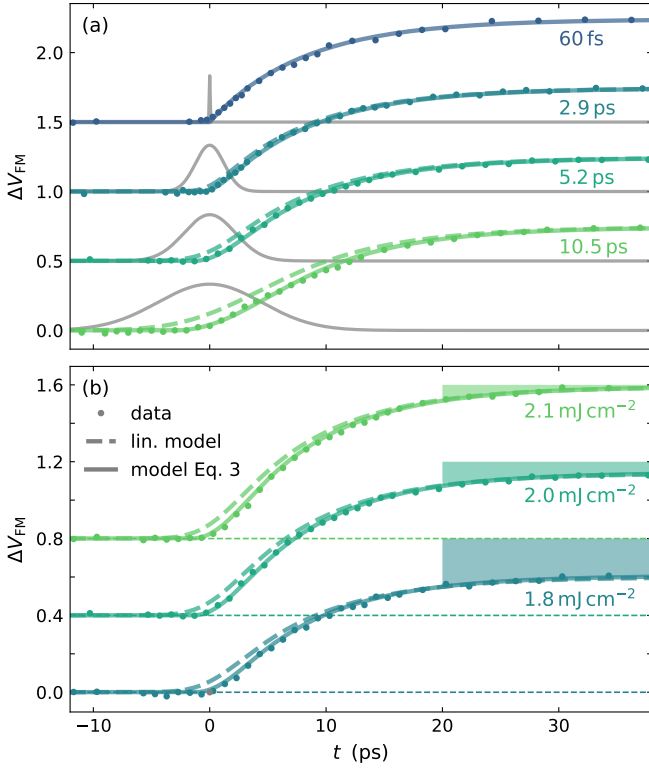


FIG. 3. **Laser-induced phase transition:** (a) Laser-induced rise of the FM volume fraction  $\Delta V_{\text{FM}}$  for different pump-pulse durations (pulse profile indicated by grey solid lines) and a fluence of  $2 \text{ mJ cm}^{-2}$ . (b) Laser-induced rise of  $\Delta V_{\text{FM}}$  for various super-threshold fluences and 5.2 ps pump-pulse duration. The coloured areas denote the fraction of the film that remains in the AFM phase. For  $2.1 \text{ mJ cm}^{-2}$  the complete film ends up in the FM phase. In both panels, the dashed lines represent the FM volume fraction according to Eq. (2), i.e. for ultrashort pulse excitation, convoluted with a Gaussian representing the duration of the respective pump-pulse. The data rise faster but starts delayed compared to the dashed lines, which assume linear response via the convolution. The solid lines show the appropriate model for the FM volume fraction according to Eq. (3), which accounts for the non-linear threshold behavior. The plots are off-set for clarity.

on the 8 ps nucleation timescale. This transiently unlocked phase transition adds to the already present FM phase driven at delays  $t < t'$ . The Heaviside function  $\mathcal{H}(t - t')$  ensures a start of the phase transition at  $t'$ . To model the transient FM volume fraction we assume a linear increase of  $V_{\text{FM}}^*$  from 0 to 1 between the fluences  $F_{\text{th}} = 0.6 \text{ mJ cm}^{-2}$  and  $2.1 \text{ mJ cm}^{-2}$ , which corresponds to a full phase transition as characterized previously<sup>11</sup>.

Under this assumption, Eq. (3) yields excellent agreement (see solid lines) with the experimentally determined transients  $\Delta V_{\text{FM}}(t)$  in Fig. 3(a and b) for various pump-pulse durations and super-threshold fluences. Our model including the critical threshold of the first-order phase transition reproduces both the delayed start of the do-

main nucleation relative to the beginning of the pump pulse for longer pump-pulses and the earlier start of the domain nucleation with increasing fluence, which highlights the central role of the threshold for the laser-induced phase transition.

In summary, we studied the laser-induced magnetostructural AFM-FM phase transition in FeRh driven by picosecond pump-pulses via UXRD. The extracted transient FM volume fraction highlights the crucial role of the threshold for the first-order phase transition in FeRh. The insensitivity of the final FM volume fraction on varying the pump-pulse duration from 60 fs up to 10.5 ps reveals that the threshold is exclusively determined by the amount of deposited energy and that the laser-induced AFM-FM phase transition does not need to proceed through the generation of hot non-equilibrium electrons. With increasing pump-pulse duration we observe an increasing deviation of the FM volume fraction from a linear response model. We successfully model the data using the intrinsic nucleation of FM domains on an 8 ps timescale, by simply considering the slow deposition of energy by picosecond pump-pulses, which successively overcomes the critical threshold that makes the phase transition dynamics nonlinear.

We acknowledge the DFG for financial support via Project-No. 328545488 – TRR 227, project A10 and the BMBF for funding via 05K22IP1. Access to the CEITEC Nano Research Infrastructure was supported by the Ministry of Education, Youth and Sports (MEYS) of the Czech Republic under the project CzechNanoLab (LM2023051).

- <sup>1</sup>M. M. Qazilbash, M. Brehm, B.-G. Chae, P.-C. Ho, G. O. Andreev, B.-J. Kim, S. J. Yun, A. Balatsky, M. Maple, F. Keilmann, *et al.*, “Mott transition in  $\text{VO}_2$  revealed by infrared spectroscopy and nano-imaging,” *Science* **318**, 1750–1753 (2007).
- <sup>2</sup>S. Roy, G. Perkins, M. Chattopadhyay, A. Nigam, K. Sokhey, P. Chaddah, A. Caplin, and L. Cohen, “First order magnetic transition in doped cef<sub>2</sub> alloys: Phase coexistence and metastability,” *Physical review letters* **92**, 147203 (2004).
- <sup>3</sup>V. Uhlíř, J. A. Arregi, and E. E. Fullerton, “Colossal magnetic phase transition asymmetry in mesoscale ferri stripes,” *Nature communications* **7**, 13113 (2016).
- <sup>4</sup>C. Baldasseroni, C. Bordel, A. Gray, A. Kaiser, F. Kronast, J. Herrero-Albillos, C. Schneider, C. Fadley, and F. Hellman, “Temperature-driven nucleation of ferromagnetic domains in ferri thin films,” *Applied Physics Letters* **100**, 262401 (2012).
- <sup>5</sup>F. Randi, I. Vergara, F. Novelli, M. Esposito, M. Dell’Angela, V. Brabers, P. Metcalf, R. Kukreja, H. A. Dürr, D. Fausti, *et al.*, “Phase separation in the nonequilibrium verwey transition in magnetite,” *Physical Review B* **93**, 054305 (2016).
- <sup>6</sup>S. De Jong, R. Kukreja, C. Trabant, N. Pontius, C. Chang, T. Kachel, M. Beye, F. Sorgenfrei, C. Back, B. Bräuer, *et al.*, “Speed limit of the insulator–metal transition in magnetite,” *Nature materials* **12**, 882–886 (2013).
- <sup>7</sup>D. Wegkamp, M. Herzog, L. Xian, M. Gatti, P. Cudazzo, C. L. McGahan, R. E. Marvel, R. F. Haglund Jr, A. Rubio, M. Wolf, *et al.*, “Instantaneous band gap collapse in photoexcited monolayer  $\text{VO}_2$  due to photocarrier doping,” *Physical review letters* **113**, 216401 (2014).
- <sup>8</sup>G. Ju, J. Hohlfeld, B. Bergman, R. J. van de Veerdonk, O. N. Mryasov, J.-Y. Kim, X. Wu, D. Weller, and B. Koopmans, “Ultrafast generation of ferromagnetic order via a laser-induced

- phase transformation in ferh thin films,” *Physical review letters* **93**, 197403 (2004).
- <sup>9</sup>I. Radu, C. Stamm, N. Pontius, T. Kachel, P. Ramm, J.-U. Thiele, H. Dürr, and C. Back, “Laser-induced generation and quenching of magnetization on ferh studied with time-resolved x-ray magnetic circular dichroism,” *Physical Review B* **81**, 104415 (2010).
  - <sup>10</sup>S. O. Mariager, F. Pressacco, G. Ingold, A. Caviezel, E. Möhr-Vorobeva, P. Beaud, S. Johnson, C. Milne, E. Mancini, S. Moyerman, *et al.*, “Structural and magnetic dynamics of a laser induced phase transition in ferh,” *Physical Review Letters* **108**, 087201 (2012).
  - <sup>11</sup>M. Mattern, J. Jarecki, J. A. Arregi, V. Uhlř, M. Rössle, and M. Bargheer, “Disentangling nucleation and domain growth during a laser-induced phase transition,” (2023), 10.48550/arXiv.2305.02094.
  - <sup>12</sup>M. Mattern, J.-E. Pudell, K. Dumesnil, A. von Reppert, and M. Bargheer, “Towards shaping picosecond strain pulses via magnetostrictive transducers,” *Photoacoustics* **30**, 100463 (2023).
  - <sup>13</sup>S. Polesya, S. Mankovsky, D. Ködderitzsch, J. Minár, and H. Ebert, “Finite-temperature magnetism of ferh compounds,” *Physical Review B* **93**, 024423 (2016).
  - <sup>14</sup>C. Kittel, “Model of exchange-inversion magnetization,” *Physical Review* **120**, 335 (1960).
  - <sup>15</sup>R. Gu and V. Antropov, “Dominance of the spin-wave contribution to the magnetic phase transition in ferh,” *Physical Review B* **72**, 012403 (2005).
  - <sup>16</sup>M. Gruner, E. Hoffmann, and P. Entel, “Instability of the rhodium magnetic moment as the origin of the metamagnetic phase transition in  $\alpha$ -ferh,” *Physical Review B* **67**, 064415 (2003).
  - <sup>17</sup>L. M. Sandratskii and P. Mavropoulos, “Magnetic excitations and femtomagnetism of ferh: A first-principles study,” *Physical Review B* **83**, 174408 (2011).
  - <sup>18</sup>J. Barker and R. W. Chantrell, “Higher-order exchange interactions leading to metamagnetism in ferh,” *Physical Review B* **92**, 094402 (2015).
  - <sup>19</sup>F. Pressacco, D. Sangalli, V. Uhlř, D. Kutnyakhov, J. A. Arregi, S. Y. Agustsson, G. Brenner, H. Redlin, M. Heber, D. Vasilyev, *et al.*, “Subpicosecond metamagnetic phase transition in ferh driven by non-equilibrium electron dynamics,” *Nature Communications* **12**, 5088 (2021).
  - <sup>20</sup>F. Quirin, M. Vattilana, U. Shymanovich, A.-E. El-Kamhawy, A. Tarasevitch, J. Hohlfeld, D. von der Linde, and K. Sokolowski-Tinten, “Structural dynamics in ferh during a laser-induced metamagnetic phase transition,” *Physical Review B* **85**, 020103 (2012).
  - <sup>21</sup>M. Mattern, J.-E. Pudell, J. A. Arregi, J. Zlámál, R. Kalousek, V. Uhlř, M. Rössle, and M. Bargheer, “Accelerating the laser-induced phase transition in nanostructured ferh via plasmonic absorption,” (2023), 10.48550/arXiv.2309.12683.
  - <sup>22</sup>B. Bergman, G. Ju, J. Hohlfeld, R. J. van de Veedonk, J.-Y. Kim, X. Wu, D. Weller, and B. Koopmans, “Identifying growth mechanisms for laser-induced magnetization in ferh,” *Physical Review B* **73**, 060407 (2006).
  - <sup>23</sup>G. Li, R. Medapalli, J. Mentink, R. Mikhaylovskiy, T. Blank, S. Patel, A. Zvezdin, T. Rasing, E. Fullerton, and A. Kimel, “Ultrafast kinetics of the antiferromagnetic-ferromagnetic phase transition in ferh,” *Nature Communications* **13**, 2998 (2022).
  - <sup>24</sup>I. Dolgikh, T. Blank, G. Li, K. Prabhakara, S. Patel, A. Buzdakov, R. Medapalli, E. Fullerton, O. Koplak, J. Mentink, *et al.*, “Ultrafast emergence of ferromagnetism in antiferromagnetic ferh in high magnetic fields,” (2022), 10.48550/arXiv.2202.03931.
  - <sup>25</sup>J. A. Arregi, O. Caha, and V. Uhlř, “Evolution of strain across the magnetostructural phase transition in epitaxial ferh films on different substrates,” *Physical Review B* **101**, 174413 (2020).
  - <sup>26</sup>M. Rössle, W. Leitenberger, M. Reinhardt, A. Koç, J. Pudell, C. Kwamen, and M. Bargheer, “The time-resolved hard x-ray diffraction endstation kmc-3 xpp at bessy ii,” *Journal of Synchrotron Radiation* **28**, 948–960 (2021).
  - <sup>27</sup>F. Pressacco, V. Uhlř, M. Gatti, A. Bendounan, E. E. Fullerton, and F. Sirotti, “Stable room-temperature ferromagnetic phase at the ferh (100) surface,” *Scientific reports* **6**, 22383 (2016).
  - <sup>28</sup>R. Fan, C. J. Kinane, T. Charlton, R. Dorner, M. Ali, M. De Vries, R. M. Brydson, C. H. Marrows, B. J. Hickey, D. A. Arena, *et al.*, “Ferromagnetism at the interfaces of antiferromagnetic ferh epilayers,” *Physical Review B* **82**, 184418 (2010).
  - <sup>29</sup>X. Chen, J. Feng, Z. Wang, J. Zhang, X. Zhong, C. Song, L. Jin, B. Zhang, F. Li, M. Jiang, *et al.*, “Tunneling anisotropic magnetoresistance driven by magnetic phase transition,” *Nature Communications* **8**, 449 (2017).
  - <sup>30</sup>M. Mattern, A. von Reppert, S. P. Zeuschner, M. Herzog, J.-E. Pudell, and M. Bargheer, “Concepts and use cases for picosecond ultrasonics with x-rays,” *Photoacoustics* , 100503 (2023).
  - <sup>31</sup>D. Schick, “udkm1dsim—a python toolbox for simulating 1d ultrafast dynamics in condensed matter,” *Computer Physics Communications* **266**, 108031 (2021).
  - <sup>32</sup>P. Tu, A. Heeger, J. Kouvel, and J. Comly, “Mechanism for the first-order magnetic transition in the ferh system,” *Journal of Applied Physics* **40**, 1368–1369 (1969).
  - <sup>33</sup>M. Richardson, D. Melville, and J. Ricodeau, “Specific heat measurements on an fe rh alloy,” *Physics Letters A* **46**, 153–154 (1973).
  - <sup>34</sup>S. Günther, C. Spezzani, R. Ciprian, C. Grazioli, B. Ressel, M. Coreno, L. Poletto, P. Miotti, M. Sacchi, G. Panaccione, *et al.*, “Testing spin-flip scattering as a possible mechanism of ultrafast demagnetization in ordered magnetic alloys,” *Physical Review B* **90**, 180407 (2014).
  - <sup>35</sup>D. Schick, R. Shayduk, A. Bojahr, M. Herzog, C. v. Korff Schmising, P. Gaal, and M. Bargheer, “Ultrafast reciprocal-space mapping with a convergent beam,” *Journal of Applied Crystallography* **46**, 1372–1377 (2013).
  - <sup>36</sup>D. Schick, A. Bojahr, M. Herzog, C. v. K. Schmising, R. Shayduk, W. Leitenberger, P. Gaal, and M. Bargheer, “Normalization schemes for ultrafast x-ray diffraction using a table-top laser-driven plasma source,” *Review of Scientific Instruments* **83**, 025104 (2012).
  - <sup>37</sup>S. Palmer, P. Dentschuk, and D. Melville, “Elastic properties of an iron-rhodium alloy,” *physica status solidi (a)* **32**, 503–508 (1975).
  - <sup>38</sup>Y. Ahn, M. J. Cherukara, Z. Cai, M. Bartlein, T. Zhou, A. DiChiara, D. A. Walko, M. Holt, E. E. Fullerton, P. G. Evans, *et al.*, “X-ray nanodiffraction imaging reveals distinct nanoscopic dynamics of an ultrafast phase transition,” *Proceedings of the National Academy of Sciences* **119**, e2118597119 (2022).